



OPTIMIZATION OF WELDING CONDITIONS ON MECHANICAL PROPERTIES FOR FRICTION WELDING OF AISI 301 STAINLESS STEEL

Muhammad Iswar^{1,2} and Rusdi Nur^{1,2}

¹Department of Mechanical Engineering, Politeknik Negeri Ujung Pandang, Makassar, Indonesia

²Center for Materials and Manufacturing, Politeknik Negeri Ujung Pandang, Makassar, Indonesia

E-Mail: muh_iswar@poliupg.ac.id

ABSTRACT

Stainless steel AISI 310 is one of the most widely used grades of heat-resistant stainless steel supplied into numerous industry sectors. The key properties of this material are its high chromium and medium nickel content making its resistance to oxidation, sulfidation and other forms of hot corrosion its main characteristics. This study investigates the influence of rotation speed and forging time during machining on responses of tensile strength and hardness. The turning was performed at various cutting speeds (550, 1020, and 1800 rpm) and forging time (25, 35, and 45 seconds). Response surface methodology was adopted in designing the experiments to quantify the effect of rotation speed and forging time on the friction welding responses. It was found that rotation speed was proportional to the tensile strength and was inversely proportional to hardness. Forging time was proportional to the tensile strength and was inversely proportional to hardness. Empirical equations developed from the results for all friction welding responses were shown to be useful in determining the optimum welding parameters range.

Keywords: friction welding; mechanical properties; stainless steel.

INTRODUCTION

Welding process is one of the metal grafting techniques. This technique is carried out by melting the parent metal and filler metal with or without pressure and additional metal to produce a continuous connection. Commonly, the metal welding technique consists of fusion welding, solid state welding, soldering, and brazing.

Friction welding is a solid-state welding process that generates heat through mechanical friction between workpieces in relative motion to one another, with the addition of a lateral force called "upset" to plastically displace and fuse the materials. Because no melting occurs, friction welding is not a fusion welding process in

the traditional sense, but more of a forge welding technique. Friction welding is used with metals and thermoplastics in a wide variety of aviation and automotive applications (Thomas *et al.*, 1995). The basic steps of the friction welding process were shown in Figure-1. The process of metal grafting that occurs due to friction due to rotation of one metal to the other and the existence of axial pressure. Friction welding has advantages such as not using added materials, uniform welding of the entire surface, maintaining material compatibility that is attached and applicable for welding on different materials (Lee *et al.*, 2004; Lee *et al.*, 2005).

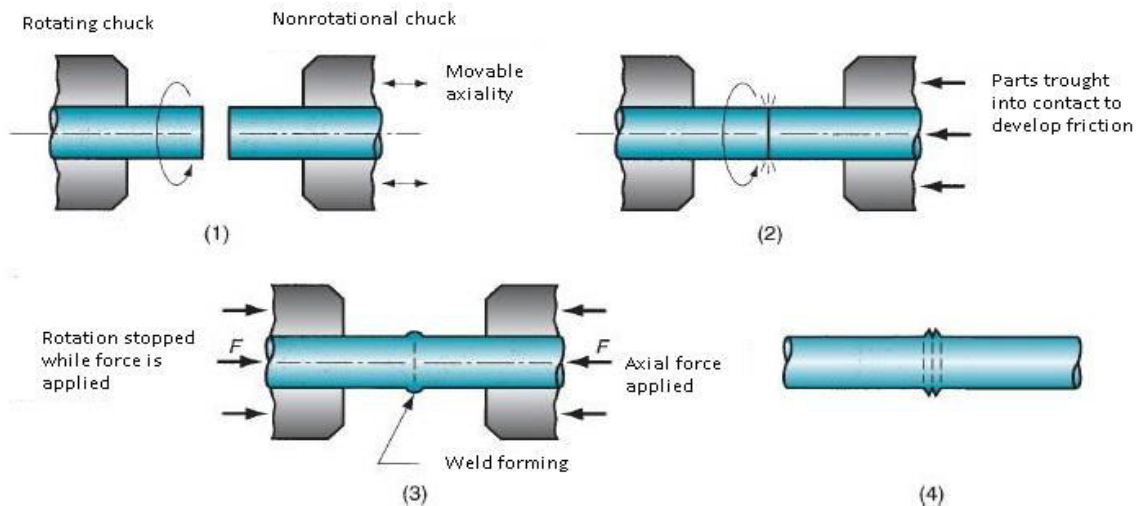


Figure-1. Working principle of friction welding, as following stages: (1) one component is positioned in a stationary chuck and the other in the rotating chuck, (2) brought up to a rotational speed and parts brought into contact to develop friction, (3) Rotating stopped while axial force is applied to occur the weld forming, (4) the two materials are plasticized (became malleable) (Nicholas, 2003; Yilbas *et al.*, 1995).

There are several physical phenomena in friction welding, such as changes due to friction, plastic deformation, solidification, structural changes and so on. The parameters in the friction welding process include friction time, rotation speed and friction pressure is shown in Figure-2.

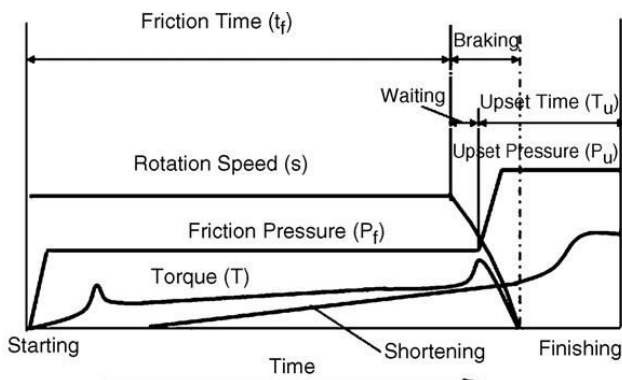


Figure-2. Working parameters of friction welding (Sathiya *et al.*, 2007).

In this experiment, stainless steel containing about 12% Cr was used. The addition of Cr causes increased rust resistance since Cr will form a thin oxide layer that can protect the metal from corrosion. The addition of Ni to this steel increases the resistance of the rust and improves the ductility and formability. Stainless Steel AISI 301 is a type of austenitic stainless steel with low carbon content. This type is made for materials with consideration of economic value, excellent for the polluted environment and in fresh water. Higher Cr will serve as a protective to increase corrosion resistance. The low carbon composition in this material can minimize sensitization due to the welding process and has a melting temperature (T_m) of 1399 - 1421°C. Based on the melting temperature

of AISI 301 stainless steel, the temperature that can be used in friction welding process was 979.3°C ($0.7 \times T_m$), is called as recrystallization temperature (T_r). The welding temperature used in this study is 850°C (below T_r), 950°C (T_r) and 1050°C (above T_r). It was performed to obtain the experimental data more accurately.

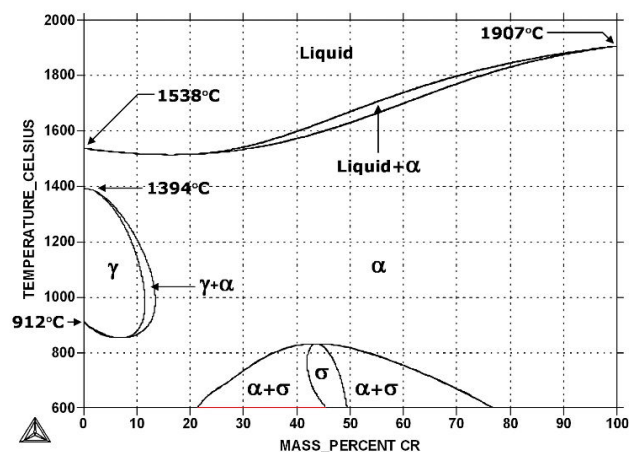


Figure-3. Fe-Cr phase diagram (Ustinovshikov *et al.*, 2002).

EXPERIMENTAL METHOD

Welding process is done by using a milling machine. The tool used was a tool formed with a lathe as in Figure-2. The material to be joined is aluminum alloy AA 5052 with 4x85x200 size. The workpiece is clamped using a clamp vice. The tool was rotated and penetrating into the workpiece. Experiments carried out by doing some initial experiments in order to obtain study variables such as the value of the round and feeding tool that can be used to connect the material and further testing the mechanical properties of the weld which includes tensile



testing, bending, hardness and SEM. There are two sizes of shoulder diameter that is used is 17.8 mm and 25 mm with a round that can be used is 855 rpm, 1300 rpm and 1950 rpm while feeding large 50 mm/min, 135 mm/min, 208 mm/min.

Materials and Machine Tool Specification

In this study, stainless steel AISI 301 was used; the material used is with size \varnothing 15.8 mm. Mechanical properties and specimen type of AISI301 are shown in Table-1 and Figure-4 respectively.

Table-1. Mechanical properties of AISI 301.

	Ultimate strength (MPa)	Yield strength (MPa)	Hardness	Elongation (%)
AISI 301 Stainless Steel	770	325	320 HV / 90 HRB	56

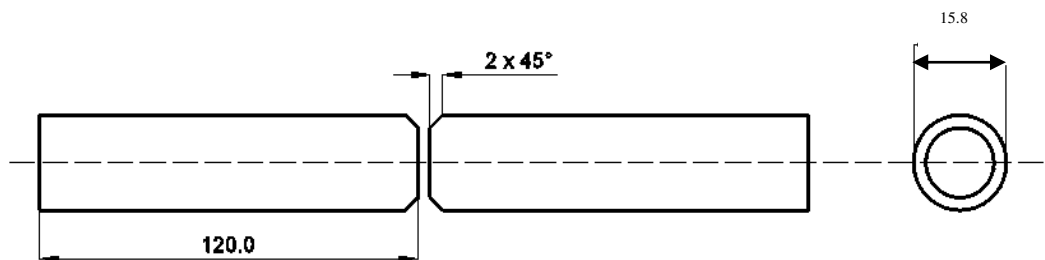


Figure-4. Specimen for welding friction.

A Pindad lathe machine was used to rotate workpieces in the friction welding process that was modified with the addition of a hydraulic system. Other equipment for measuring instruments is infrared thermometer, stopwatch, tensile testing machine (UTM Galdabini), and hardness testing machine (Harness Rockwell Cone). Hardness tester (Affri MX 206) was used to determine the hardness that varies throughout the welding zone.

Friction Welding Parameters

Process parameters that affect the characteristics of turned parts are rotation speed, forging time and pressure, and friction pressure. These parameters depend on the workpiece material and the machine tool chosen to perform the turning operation. The parameters used were shown in Table-2.

Table-2. The parameters used in the friction welding experiments.

Item	Parameters
Stainless Steel AISI 301, d(mm)	15.8
Rotation speed, S_1, S_2, S_3 (rpm)	550, 1020, 1800
Forging time, Ft_1, Ft_2, Ft_3 (s)	25, 35, 45
Forging pressure, P_u (MPa)	123.8
Friction Pressure, P_f (MPa)	82.1

AISI 301 stainless steel workpiece was cut in accordance with predetermined dimensions. The workpiece is clamped on a rotating spindle and the other side is clamped to the fixed jaw. At the beginning of the rotation speed, the friction pressure should start from the lowest pressure till increased to create the heat caused by friction. When the welding temperature has been reached (1050°C), the rotation speed is stopped and the forging pressure is applied while holding the pressure at the desired wrought time.

For each experimental design data, the friction welding process is carried out repeatedly by varying several welding parameters such as rotation and the forging time. The friction welding process is carried out on a Pindad lathe using a pressure-suppression mode by a tail-stock equipped with the addition of a pressure gauge using a hydraulic system as illustrated in the Figure-5.

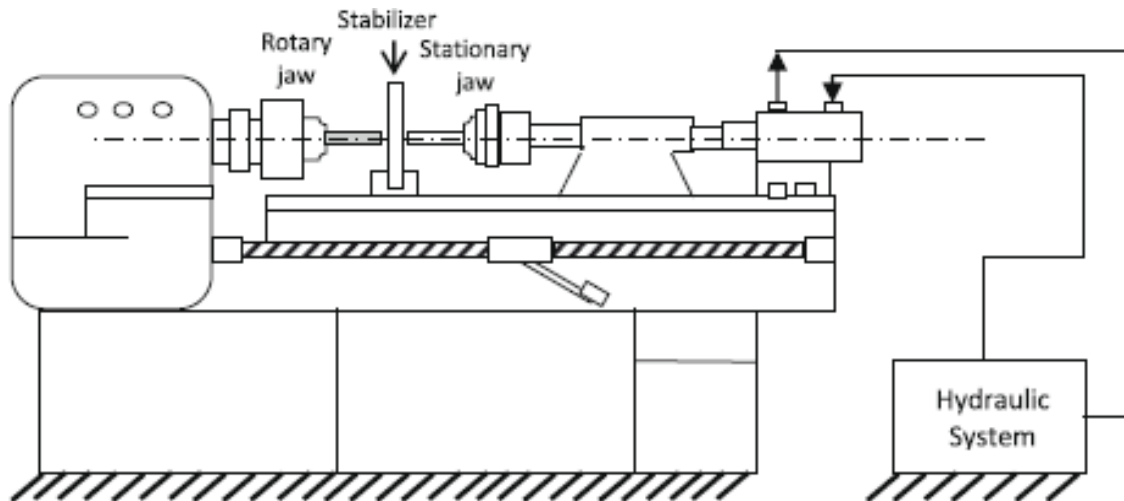


Figure-5. Friction welding process using a turning machine.

The experimental was optimized for the machining conditions using the centered cubic design method.

Tensile Strength and Hardness Measurement System

After the welding process, the welding workpiece is formed into a specimen for mechanical testing, namely:

tensile test and hardness test. The tensile testing was performed using a Galdabini Universal Testing Machine with 10-ton capacity. The type specimen for tensile strength have size according to ISO 82-1974 (E), DP8, $l_0 = 80$ mm, as shown in the following figure.

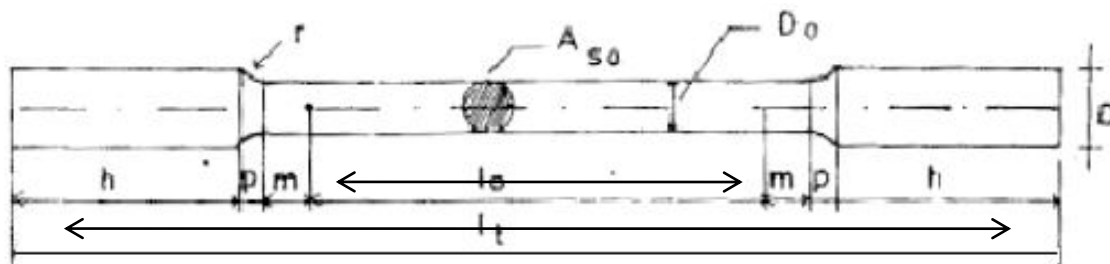


Figure-6. Specimen for the tensile test.

Hardness testing using the Rockwell Cone method by using pyramidal diamonds with 120° peak angles loaded with F loads. Rockwell's hardness testing is based on the depth of emphasis on the material under test. The depth of stress entry indicates the hardness value of the test material shown directly in the dial panel after the main load is released and the initial load still withstands the load. The area tested for hardness is in the weld area (1 point), Heat Affected area (HAZ) (4 points), and the parent metal (2 points).

- Rockwell Cone Scale A
- 120° of Penetrator
- Load of 558 N
- Loading time is 10 second

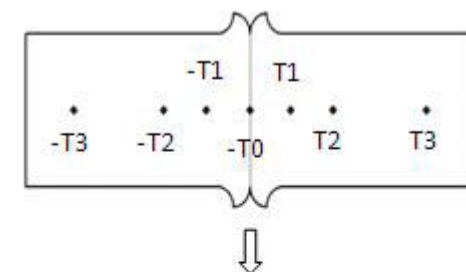


Figure-7. Location for hardness testing.

**Table-3.** The hardness test result.

Parameters		HRC-A (Newton)						
Rotation speed	Forging time	Raw material	HAZ	HAZ	Welds area	HAZ	HAZ	Raw material
(rpm)	(s)	(-T3)	(-T2)	(-T1)	(T0)	(T1)	(T2)	(T3)
550	25	68,2	66,7	61,7	61,5	61,3	66,5	67,7
	35	69,0	58,8	59,0	57,2	58,6	65,8	67,9
	45	68,9	58,7	58,0	57,0	58,0	62,8	68,5
1020	25	68,2	63,1	60,6	60,3	62,9	67,8	68,3
	35	68,0	66,7	59,3	57,5	59,7	65,9	67,9
	45	68,3	62,5	58,4	58,1	58,2	58,5	68,5
1800	25	69,7	64,5	61,6	59,5	61,8	68,1	69,7
	35	69,2	59,2	58,9	58,3	58,7	56,2	67,5
	45	66,7	63,0	59,2	60,5	59,7	67,7	68,0

RESULTS AND DISCUSSIONS

For each machining response, an empirical model was developed according to guidelines for a three-level full factorial design with two repetitions at the center

point, which were established elsewhere (Nur *et al.*, 2017). A total of nine runs are included in the design of experiment, and the results are shown in Table-4.

Table-4. Design layout and experimental results.

Std.	Rotation Speed (S)	Forging Time (t)	Coded		Tensile Strength (Ts)	Hardness
	[rpm]	[s]	x_1	x_2	MPa	(HRC)
1	550	25	-1	-1	477.70	61.5
2	1020	25	0	-1	533.44	60.3
3	1800	25	1	-1	650.90	59.5
4	550	35	-1	0	533.44	57.2
5	1020	35	0	0	607.10	57.5
6	1800	35	1	0	656.85	58.3
7	550	45	-1	1	583.20	57.0
8	1020	45	0	1	621.02	58.1
9	1800	45	1	1	706.61	60.5

Tensile Strength

Results of tensile strength show that it fits the linear model for various rotation speeds and forging time. The ANOVA for the tensile strength data is given in Table-5. Having its Prob>F of much less than 0.01, the

linear model is valid. As for the coefficients, both of the rotation speeds and forging time was considered as a significant factor. Tensile strength was insensitive to the change in rotation speeds and forging time.



Table-5. ANOVA analysis for linear of the tensile strength.

Source	Sum of squares	DOF	Mean Square	F Value	Prob > F
Model	40106.96	2	20053.48	76.37	<0.0001
x ₁	29790.88	1	29790.88	113.46	<0.0001
x ₂	10316.08	1	10316.08	39.29	0.0008
Residual	1575.44	6	262.57		
Core total	41682.40	8			

The obtained empirical equation of tensile strength (Ts) in the form of actual factor is as stated in equation (1),

$$T_s = +326.19971 + 0.11160 * S + 4.14650 * t \quad (1)$$

Where *S* is rotation speed (rpm) and *t* is forging time (s).

For convenience, the equation can be displayed as response surface contour as well as three-dimensional surfaces, as shown in Figure-8.

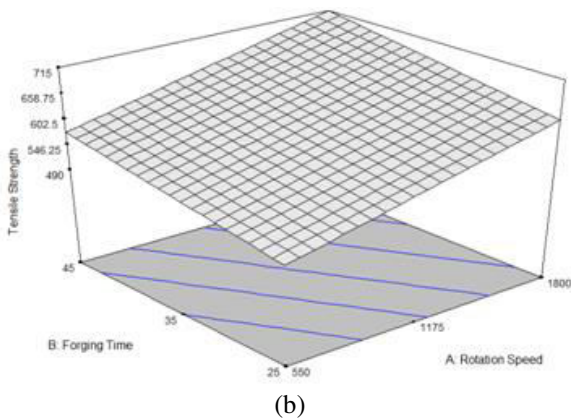
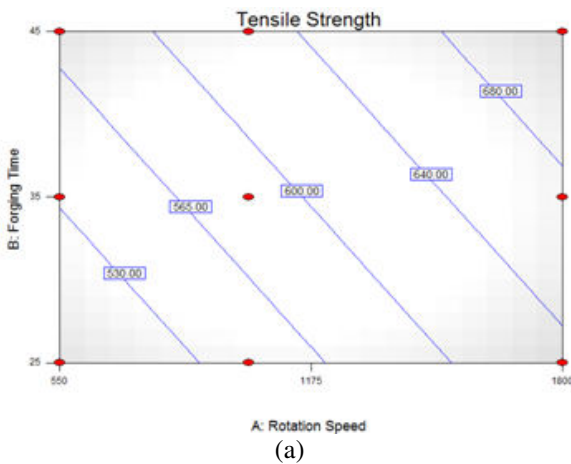


Figure-8. Response surface graph of (a) contours and (b) 3D Surface for tensile strength.

The tensile test result data showed that the highest maximum tensile stress (706.61 N/mm²) was obtained at 1800 rpm and 45 s of forging time with a strain of 7.72%. The lowest tensile strength (477.7 N/mm²) was obtained at 550 rpm and 25 seconds of wrought time with

1.8% of strain. Figure-8 shows clearly that the tensile strength of friction welding has similarity to the raw material. The highest tensile strength ratio of welding result shows the difference of tensile stress about 73, 6 N/mm² and the difference of strain 28, 4%. The percentages of tensile strength decrease about 9.4% and strain about 78.6%. It can be concluded that the strength of the welding results is almost equal to the strength of the raw material, but all the welded specimens have a failure in the welded joint area. Ozdemir (2005) has performed the friction welding of AISI 304L/4340. The experimental results indicate that the tensile strength of friction-welded 304L/4340 components was markedly affected by joining rotational speed selected (Hascalik *et al.*, 2006). The low strain value indicates that the specimen of welding friction has a more brittle connective nature although basically, the raw material is tough. The fracture has a brittle form, which means the fracture strength is almost equal to its maximum strength, as shown in Figure-8. Sathiya *et al.* (2007) had been investigated the mechanical properties on friction welding of stainless steel AISI 430, including the tensile and impact strength, hardness, and also microstructural aspects. The friction welding of stainless steel AISI 430 was successfully join and exhibited better mechanical characteristics, such as 90 - 95 % for parent material's tensile strength.

Table-6. After tensile test for 15.8 mm of diameter (P_u: 123.8 MPa, 1800 rpm / 45s).

Temperature	The shape after tensile test
850° C	85 % solid
950° C	90 % solid
1050° C	97 % solid



Hardness

Results for hardness show that it fits the quadratic model for rotation speeds and forging time. The ANOVA for the hardness data is given in Table-7. Having its

Prob>F of much less than 0.01, the quadratic model is valid. As for the coefficients, the rotation speeds and forging time was considered as a significant factor.

Table-7. ANOVA analysis for quadratic of the hardness.

Source	Sum of squares	DOF	Mean Square	F Value	Prob > F
Model	20.89	4	5.22	102.56	0.0003
x_1	1.26	1	1.26	24.82	0.0076
x_2	4.16	1	4.16	81.74	0.0008
x_2^2	6.60	1	6.60	129.62	0.0003
$x_1 x_2$	7.61	1	7.61	149.49	0.0003
Residual	0.20	4	0.051		
Core total	21.10	8			

The obtained empirical equation of the hardness in the form of actual factor is as stated in equation (2),

$$\text{Hardness} = +91.02 - 6.92\text{E-}003*S - 1.61 * Ft + 0.02 * t^2 + 2.18497\text{E-}004*S*t \quad (2)$$

Where S is rotation speed (rpm) and t is forging time (s).

For convenience, the equation can be displayed as response surface contour as well as three-dimensional surfaces, as shown in Figure-9.

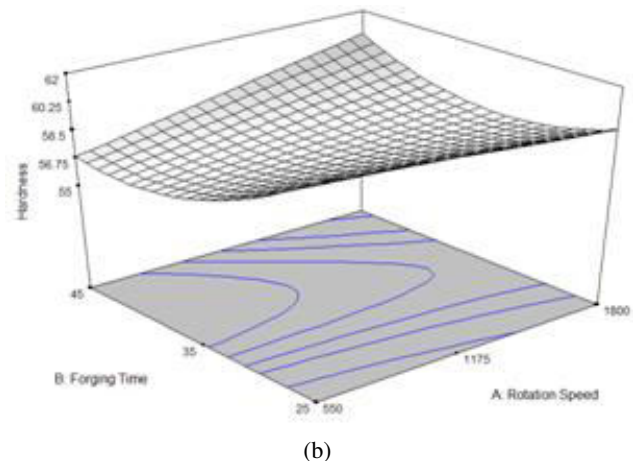
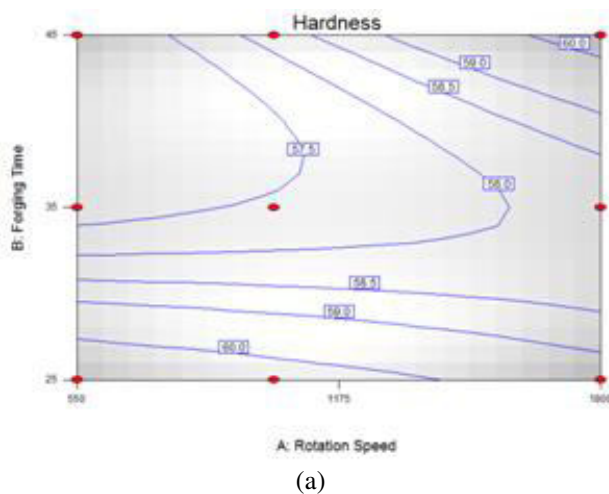


Figure-9. Response surface graph of (a) contours and (b) 3D Surface for hardness.

Figure-9 shows the hardness of welded joints and the HAZ decreases if the forging time is longer, but the hardness value increases if the lower the temperature. It also occurs in specimens with variations of 1020 rpm and 1800 rpm. The higher hardness was obtained on 1800 rpm of rotation speed and 45 seconds. The difference in hardness values on welded joints is not very large, ranging from 1-8 HRC-A. The same welding temperature that is 1050°C is the factor causing the hardness value of welded joint which is not much different. Hasçalik *et al.* (2006) were investigated the friction welding of AISI 304/4340. The Vickers microhardness distributions in the welding zone were determined. The experimental results indicate that mechanical properties are affected significantly by rotation speed and the fatigue strength of friction-welded samples decrease due to chromium carbide precipitation in welding zone with increasing rotation speed in chosen conditions (Hasçalik *et al.*, 2006). Another experiment by Ates *et al.*, they have investigated the influence of friction pressure through tensile strength and hardness and also determined the optimum friction pressure (Ates *et al.*, 2007).



Optimization

The empirical models for all responses (i.e. hardness and tensile strength) have been obtained, thus selecting the optimum conditions (i.e. rotational speed and forging time) can be done. It was expected the range for each machining parameters, thus it can determine all machining response that fit the expectation. This can determine the desired limit, namely the tensile strength must be more than 650 MPa and the hardness must be less than 56.5 HRC. For example, determining the desired limit, namely the tensile strength shall be more than 650 MPa and the hardness shall be less than 56.5 HRC. To achieve those criteria, the range of rotation speed and forging time should fall within the gray region of the overlay plot (Figure-10) of all the responses.

Rizvi and Tewari (2017) were optimized the welding parameters using Taguchi-grey relational analysis through gas metal arc-welding of AISI 304 stainless steel. Sathiya *et al.* (2009) was investigated the welding parameters in friction welding of AISI 304 stainless steel and was optimized using the artificial neural network (ANN) and non-conventional methods. Khalilpourazary and Payam (2016) were also used ANOVA and grey relational analysis to optimize warpage and shrinkage when the injection molding process of Derlin 500 composite.

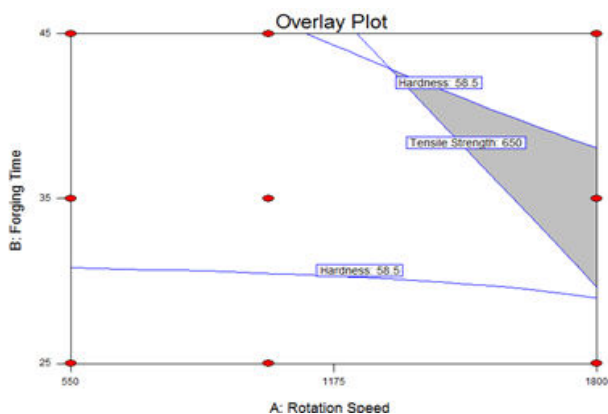


Figure-10. Overlay plot of the input factors for the predetermined response criteria of minimum of 58.5 HRC of hardness and 650 MPa of tensile strength.

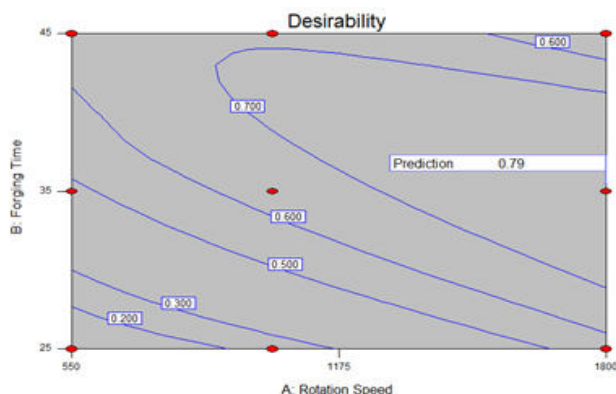


Figure-11. Desirability plots of the input factors to obtain the minimum of hardness and the tensile strength.

Another way to use the empirical equations of the responses is for determining the optimum conditions when a set of machining response is desired. Figure-11 shows the graphical optimization of the so-called desirability plot when one wishes to determine the optimum cutting speed and feed which will result in the minimum of tensile strength and hardness. For such target, the optimum conditions combination is at forging time of 35 second and rotation speed of 1800 rpm.

CONCLUSIONS

Based on the results of experiment and analysis, it can be concluded that:

- The lower the friction temperature increases the hardness value. The rotation variation influences the hardness value, the higher the engine speed increases the hardness value. In contrast to the variation of wrought time, the longer forging time will make the lower hardness value.
- For the tensile strength response, it shows that the higher the rotation speed will increase the tensile strength as well as the longer forging time. The tensile strength of welding results is almost equal to the raw material.

ACKNOWLEDGEMENTS

We are thankful to Mechanical Engineering Department and Politeknik Negeri Ung Pandang. This paper was founded by the Fundamental Research of Politeknik Negeri Ung Pandang (Project No. 388/PL10/PL/2018).

REFERENCES

- [1] Thomas W.M., Nicholas E.D., Needham J.C., Murch M.G., Temple-Smith P. and Dawes C.J. 1995. Welding Institute England, Friction Welding. U.S. Patent. 5, 460, 317.
- [2] Lee W.B., Kim Y.J. and Jung S.B. 2004. Effects of copper insert layer on the properties of friction welded joints between TiAl and AISI 4140 structural steel. *Intermetallics*. 12(6): 671-678.
- [3] Lee W.B., Bang K.S. and Jung S.B. 2005. Effects of intermetallic compound on the electrical and mechanical properties of friction welded Cu/Al bimetallic joints during annealing. *Journal of Alloys and Compounds*. 390(1-2): 212-219.
- [4] Nicholas E.D. 2003. Friction processing technologies. *Welding in the World*. 47(11-12): 2-9.
- [5] Yilbaş B.S., Şahin A.Z., Kahraman N. and Al-Garni A.Z. 1995. Friction welding of St₁ Al and Al₁ Cu materials. *Journal of Materials Processing Technology*. 49(3-4): 431-443.



- [6] Sathiya P., Aravindan S. and Haq A.N. 2007. Effect of friction welding parameters on mechanical and metallurgical properties of ferritic stainless steel. *The International Journal of Advanced Manufacturing Technology*. 31(11-12): 1076-1082.
- [7] Ustinovshikov Y., Pushkarev B. and Igumnov I. 2002. Fe-rich portion of the Fe-Cr phase diagram: electron microscopy study. *Journal of materials science*. 37(10): 2031-2042.
- [8] Nur R., Noordin M.Y., Izman S. and Kurniawan D. 2017. Machining parameters effect in dry turning of AISI 316L stainless steel using coated carbide tools. *Proceedings of the Institution of Mechanical Engineers, Part E: Journal of Process Mechanical Engineering*. 231(4): 676-683.
- [9] Özdemir N. 2005. Investigation of the mechanical properties of friction-welded joints between AISI 304L and AISI 4340 steel as a function rotational speed. *Materials Letters*. 59(19-20): 2504-2509.
- [10] Hasçalik A., Ünal E. and Özdemir N. 2006. Fatigue behavior of AISI 304 steel to AISI 4340 steel welded by friction welding. *Journal of materials science*. 41(11): 3233-3239.
- [11] Ates H., Turker M. and Kurt A. 2007. Effect of friction pressure on the properties of friction welded MA956 iron-based superalloy. *Materials & design*. 28(3): 948-953.
- [12] Rizvi S.A. and Tewari S.P. 2018. Optimization of gas metal arc-welding parameters of SS304 austenitic steel by Taguchi-Grey relational analysis. *Journal of Computational and Applied Research in Mechanical Engineering (JCARME)*. 7(2): 189-198.
- [13] Sathiya P., Aravindan S., Haq A.N. and Paneerselvam K. 2009. Optimization of friction welding parameters using evolutionary computational techniques. *Journal of materials processing technology*. 209(5): 2576-2584.
- [14] Fauzi M.A., Uday M.B., Zuhailawati H. and Ismail A.B. 2010. Microstructure and mechanical properties of alumina-6061 aluminum alloy joined by friction welding. *Materials & Design*. 31(2): 670-676.
- [15] Khalilpourazary S. and N. Payam. 2016. Optimization of the injection molding process of Derlin 500 composite using ANOVA and grey relational analysis. *Journal of Computational & Applied Research in Mechanical Engineering*. 6(1): 39-50.